

Effect of Al doping and deposition runs on structural and optical properties of In_2S_3 thin films grown by CBD

M. Kilani · B. Yahmadi · N. Kamoun Turki ·
M. Castagné

Received: 5 December 2010 / Accepted: 1 April 2011 / Published online: 22 April 2011
© Springer Science+Business Media, LLC 2011

Abstract $\beta\text{-In}_{2-x}\text{Al}_x\text{S}_3$ thin films have been grown on glass substrate by chemical bath deposition for different value of Al concentration $y = ([\text{Al}]/[\text{In}])_{\text{sol}}$ ($0 \leq y \leq 5$ at.%). Samples have been characterized using X-ray diffraction, atomic force microscopy and by spectrophotometric measurements. The influence of the increase of y ratio in the structural and optical properties are described and discussed in terms of crystallinity improvement. In order to increase film thickness of $\beta\text{-In}_{2-x}\text{Al}_x\text{S}_3$, we have been realized multi-deposition system. The structural, the surface morphology as well as the optical properties seem to be improved as the film thickness is of about 1200 nm.

Introduction

Indium sulfide is an important material for optoelectronic and photovoltaic application and it is a promising candidate for many technological applications due to its stability, relatively wider band gap, and photoconductive behavior [1–3]. In_2S_3 is considered as a promising buffer layer in solar cells. It can be used as an effective nontoxic substitute for cadmium sulfide (CdS) in $\text{Cu}(\text{In},\text{Ga})\text{Se}_2$ based solar cells. The important aim of research efforts on $\beta\text{-In}_2\text{Al}_x\text{S}_3$:Al material is to improve light transmission in the blue wavelength region by using a material having wider band

gap than that of CdS. $\text{Cu}(\text{In},\text{Ga})\text{Se}_2$ based on solar cells, prepared with chemical bath deposition (CBD) and In_2S_3 used as the buffer layer, could reach efficiency (11.7%) near to that of standard cells with CdS buffer layer [4]. Various methods such as spray pyrolysis [5], ultrasonic dispersion [6], CBD [7, 8], physical vapor deposition [9], etc., have been used to prepare In_2S_3 . Among these methods, CBD is selected in the present study to prepare $\beta\text{-In}_{2-x}\text{Al}_x\text{S}_3$ CBD thin films because this technique has many advantages such as simplicity, large area films with good uniformity, low cost, etc.

In_2S_3 is an n type semiconductor, existing in three crystallographic phases α , β , and γ . Among these structures, $\beta\text{-In}_2\text{S}_3$ which is the most stable phase at room temperature crystallizes in a normal spinel structure with a high degree of tetrahedral and octahedral vacancy sites [10–13]. Due to large number of cationic vacancies indium sulfide may be acting as a sink for aluminum incorporation. It is previously reported that the introduction of aluminum in $\beta\text{-In}_2\text{S}_3$ grown by spray pyrolysis improves the crystallinity, reduces the default of grains and reinforces contact at the boundaries grains [14].

The principal aim of this work is to study the influence of aluminum concentration $y = ([\text{Al}]/[\text{In}])_{\text{sol}}$ ($0 \leq y \leq 5$ at.%) on physical properties of $\beta\text{-In}_{2-x}\text{Al}_x\text{S}_3$ prepared by CBD. Thus, in order to increase the thickness of $\beta\text{-In}_{2-x}\text{Al}_x\text{S}_3$, the effect of multi-depositions on the physical properties for the layer obtained for the optimum Al atomic percentage $y = 4$ at.% has been studied.

Experimental details

In_2S_3 thin films are deposited via the CBD process by means of an aqueous solution containing indium

M. Kilani (✉) · B. Yahmadi · N. Kamoun Turki
Laboratoire de Physique de la Matière condensée, Faculté des
Sciences de Tunis, Tunis El Manar 2092, Tunisia
e-mail: mouna_kilani@yahoo.fr

M. Castagné
Institut d'Electronique du Sud, Université de Montpellier II,
Sciences et Techniques du Languedoc, case courrier 083. Place
Eugène BATAILLON, 34 095 Montpellier cedex 05, France

trichloride, InCl_3 (0.025 M) and thioacetamide, TA (0.10 M) as indium and sulfur precursors, respectively [15]. We introduced an amount of aluminum within the indium sulfide. The compound source of incorporation is aluminum chloride. The atomic percentage ratios of Al in solution, represented by the ratio y ($y = [\text{Al}^{3+}]/[\text{In}^{3+}]_{\text{sol}}$), has different atomic percentage value: 0, 1, 2, 3, 4, and 5 at.%. The pH of the solution is adjusted to 2.0 and the temperature of the reaction mixture is kept constant at 70 °C. The deposition time is $t_d = 45$ which cannot exceed this value otherwise the crystallinity of thin films became poor [15]. To study the effect of Al introduction, thin films of $\text{In}_{2-x}\text{Al}_x\text{S}_3$ using different atomic percentage ratios y have been prepared.

First, the layer structure is studied by X-ray diffraction (XRD) using an automated Bruker D8 advanced X-ray diffractometer with Cu K α radiation for 2θ values ranging from 20° to 70°. Second, the surface morphology of all thin layers were investigated by electronic scanning microscopy (SEM, EDAX XL 30 (S.E)) as well as by means of atomic force microscopy (AFM, standard Veeco Dimension 3100, used in tapping mode). On the other hand, the optical transmittance was obtained using Perkin Elmer lambda 950 spectrophotometer in the wavelength range 250–2500 nm. Finally, the film thickness was measured by Dektak 3 profilometer.

Results and discussions

Al concentration effect on structural properties

XRD measurements are performed to investigate the change in the crystal structure of the film grown by CBD for different value of y ($y = ([\text{Al}]/[\text{In}])_{\text{sol}}$ 0, 1, 2, 3, 4, and 5 at.%). Figure 1 shows the XRD patterns of the indium sulfide thin films deposited on glass substrates for different atomic percentage y ($0 \leq y \leq 5$ at.%). From this figure, it can be seen that for $y = 0, 4$, and 5 at.%, the corresponding film diffractograms reveal two small peaks at approximately 33.6° and 48.0° assigned to (400) and (440) reticular planes, respectively, which characterize in cubic phase of $\beta\text{-In}_{2-x}\text{Al}_x\text{S}_3$ material (PDF-32-0456) and the best crystallinity is especially obtained for $y = 4$ and 5 at.%. Similar behavior was observed by Kamoun et al. [14] who reported that Al improves the crystallinity in same $\beta\text{-In}_{2-x}\text{Al}_x\text{S}_3$ compounds. However, at $y = 1, 2$, and 3 at.% of Al, the spectra shows clearly that the crystallinity of $\beta\text{-In}_{2-x}\text{Al}_x\text{S}_3$ is amorphous (Fig. 1). This phenomenon was observed by Couzinié-Devy et al. who reported that $\beta\text{-In}_{2-x}\text{Al}_x\text{S}_3$ thin films grown by co-evaporation become amorphous when x increases from 0.06 to 0.2 at.% [16]. For thin layers grown for different y value the thickness is found lying in (315, 410) nm domain, Table 1. We point out the fact that the increase of y is the

origin of increasing film thickness of $\beta\text{-In}_{2-x}\text{Al}_x\text{S}_3$. Moreover, the average grain ' D ' calculated using Debey-Scherrer formula [17] is also shown in Table 1. One can then notice that there is a considerable variation of ' D ' with aluminum introduction. This parameter increases from 11.2 nm for $y = 0$ at.% to 28.9 nm for $y = 4$ and 5 at.%, which can be explained that introducing Al atoms can occupy substitution in crystalline. If Al atom is similar in size to the atom of the recipient, then it is likely to be soluble and it is essential for this atom to have a moderate solubility to be an effective substitute. However, when $y = 1, 2$, and 3 at.% the introduction of aluminum within In_2S_3 thin films hinders the crystallite size so in this case Al element might not occupy the appropriate sites inside the indium sulfide. It can rather occupy interstitial positions and then deforms the crystal structure. Similar behavior was reported by Couzinié-Devy et al. who found that the decrease of the grain size of $\beta\text{-In}_{2-x}\text{Al}_x\text{S}_3$ with the increase of Al concentration is due to the formation of stress induced by different ion size [16].

The surface topography of $\beta\text{-In}_{2-x}\text{Al}_x\text{S}_3$ thin films is investigated by atomic force microscopy (AFM). Figure 2 shows AFM images of $\beta\text{-In}_{2-x}\text{Al}_x\text{S}_3$ obtained for different atomic percentage ratios of Al content " y ". For values $y = 1, 2$, and 5 at.%, the surface topographies show irregular grain sizes, we can notice the presence of islands on the surface. At $y = 4$ at.%, the surface homogeneity of the layers is practically covered with equal sized grains that are uniformly distributed and the grains on the film surface seem more homogenous and have dense structure. We can observe that RMS roughness values (listed in Table 1) vary with the increase of y ratio $[\text{Al}]/[\text{In}]$ especially for $\beta\text{-In}_{2-x}\text{Al}_x\text{S}_3$ thin film prepared using $y = 5$ at.%. For this film, it can be seen an obvious reappearance of big islands. These observations are interesting and can inform us on the nucleation during the growth. The correlation between structural and morphological analysis allow us to conclude that the best crystallinity and the better homogeneity are obtained for $\beta\text{-In}_{2-x}\text{Al}_x\text{S}_3$ thin film deposited with $y = 4$ at.%.

Al concentration effect on optical properties

Transmission measurements in the wavelength range, 250–2500 nm is performed to investigate the effect of Al content on the optical performances of window layers $\beta\text{-In}_{2-x}\text{Al}_x\text{S}_3$ thin films deposited on glass. Figure 3 shows that all obtained layers reveal good transmission in transparency region. A high transmission ($T \approx 78\%$) is reached for $\beta\text{-In}_{2-x}\text{Al}_x\text{S}_3$ thin film prepared using $y = 4$ at.%. However, the transmission value decreases to 63% for $y = 3$ at.% and vary between these two values for other ratios (0, 1, 2, and 5 at.%). We note the presence of a broad peak in the range of 450–650 nm for films prepared using

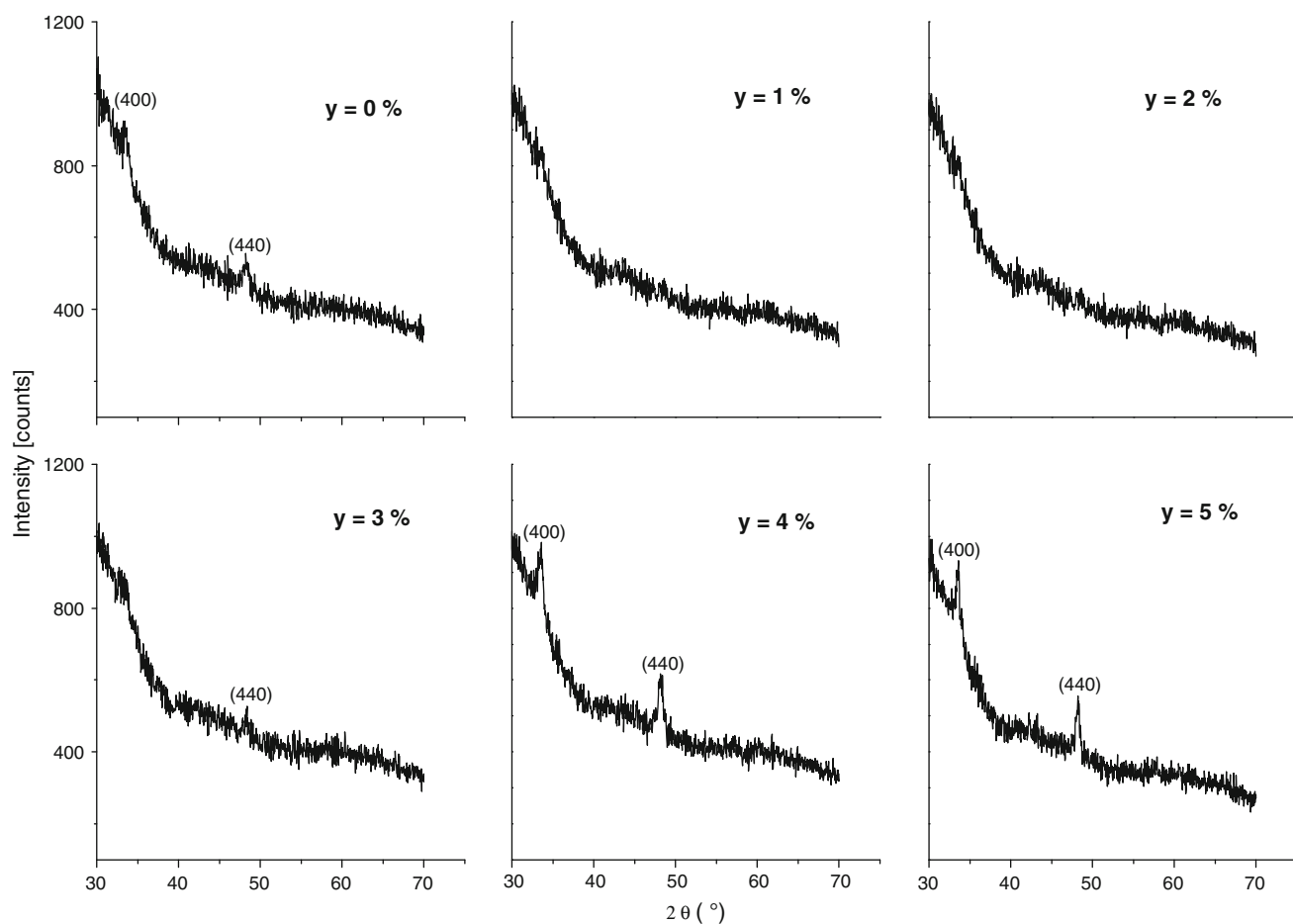


Fig. 1 X-ray spectra of monolayer β -In₂S₃ thin films deposited on glass for different atomic percentage ratios y ($y = [\text{Al}^{3+}]/[\text{In}^{3+}]_{\text{sol}}$)

Table 1 Film thickness, particle size, average roughness, and band gap energies for monolayer β -In_{2-x}Al_xS₃, Al_xS₃ deposited on glass and realized for different atomic percentage ratios y ($y = [\text{Al}^{3+}]/[\text{In}^{3+}]_{\text{sol}}$)

y	Thickness (nm)	D (nm)	RMS (nm)	Direct band gap E_g (eV)	Indirect band gap E_g (eV)
0%	315	11.2	35.9	2.50	—
1%	340	—	38.7	2.30	1.97
2%	365	—	43.2	2.32	1.95
3%	385	—	42.8	2.60	—
4%	400	28.9	41.8	2.90	—
5%	410	28.9	64	2.38	2.08

$y = 3$ and 4 at.%, it can be assigned to the excitonic peak which is more pronounced for $y = 4$ at.%. This can be revealed a good purity of thin layer grown on glass substrate using $y = 4$ at.% as an appropriate doping. Consequently, the introduction of aluminum (for $y = 4$ at.%) in the monolayer of β -In₂S₃ shows an increase of the transmission value as well as in the intrinsic absorption edge. The band gap energy E_g of all films was determined from their transmission spectra. We applied the models for both direct and indirect allowed transitions between parabolic energy bands [18]. We plotted in Fig. 4 the spectra $(\alpha h\nu)^2$

versus $(h\nu)$ (direct transitions) for all layers and $(\alpha h\nu)^{1/2}$ versus $(h\nu)$ (indirect transitions) for $y = (1, 2, \text{ and } 5 \text{ at.})$ where α is the absorption coefficient and $h\nu$ is the photon energy. The optical band gap energy can be determined by extrapolating the linear part to the region of the absorption edge. It can be observed that for curves corresponding to $y = 0, 3, \text{ and } 4$ at.%, one slope that varies with y which corresponds to the value of the direct absorption in β -In_{2-x}Al_xS₃. On the contrary, for other β -In_{2-x}Al_xS₃ thin films deposited with y equal to $1, 2, \text{ and } 5$ at.%, we note the presence of a second slope which may be due to another

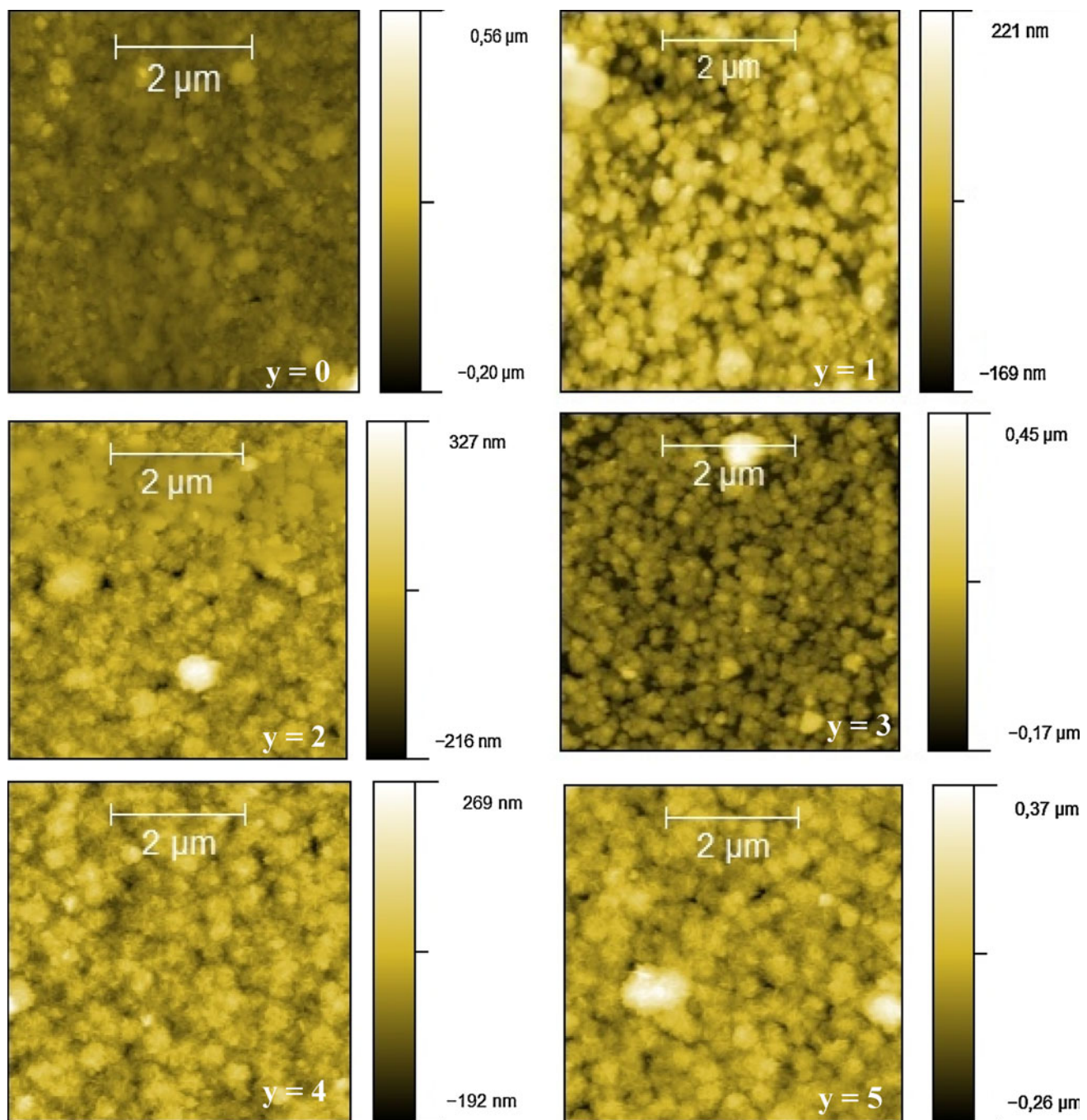


Fig. 2 AFM pictures of monolayer $\beta\text{-In}_{2-x}\text{Al}_x\text{S}_3$ deposited on glass for different atomic percentage ratios of Al ($y = [\text{Al}^{3+}]/[\text{In}^{3+}]_{\text{sol}}$)

band gap. In fact, for films prepared at y equal to 1, 2, and 5, this slope is well represented by the curves (Fig. 4), similar behavior was observed by Sandoval et al. [19]. From Table 1, it is clearly shown that the direct band gap does not linearly increase with y ; it varies from 2.30 to 2.90 eV. The wider direct band gap E_g is obtained for $y = 4$ at.% ($E_g \approx 2.90$ eV), this is a good value for use of $\beta\text{-In}_{2-x}\text{Al}_x\text{S}_3$ material as an optical window in photovoltaic

devices like $\beta\text{-In}_{2-x}\text{Al}_x\text{S}_3/\text{CuInS}_2$ or $\beta\text{-In}_{2-x}\text{Al}_x\text{S}_3/\text{SnS}$, where the compounds CuInS_2 and SnS can act as an absorber material in solar cell.

However, for allowed indirect transition, a slightly variation of the band gap with Al concentration y (1, 2, and 5 at.%) is observed in Table 1, it varies from 1.95 to 2.08 eV. Similar result was also observed by Couzinié-Devy et al. [17] who reported that the band gap

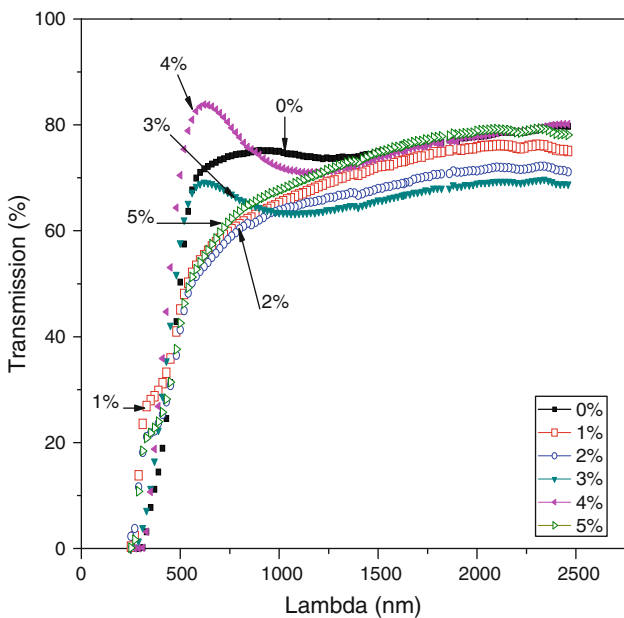


Fig. 3 Transmittance (T) spectra of monolayer $\beta\text{-In}_{2-x}\text{Al}_x\text{S}_3$ deposited on glass and realized for different atomic percentage ratios y ($y = [\text{Al}^{3+}]/[\text{In}^{3+}]_{\text{sol}}$)

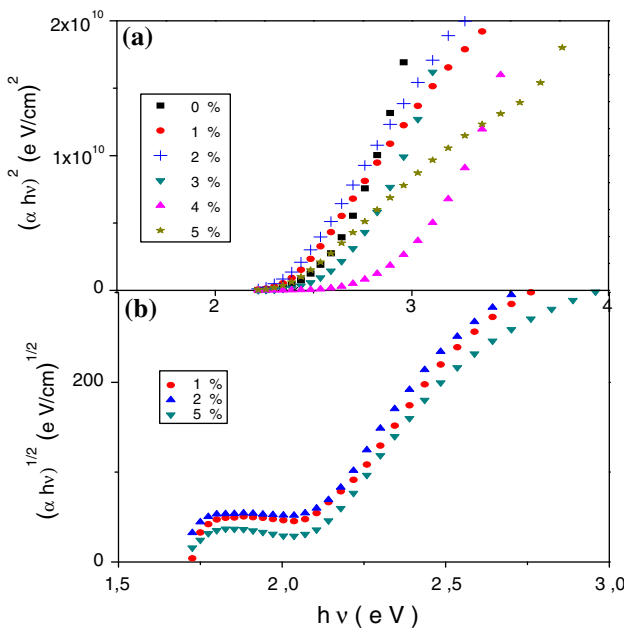


Fig. 4 **a** $(\alpha h\nu)^2$ versus $(h\nu)$ spectra and **b** $(\alpha h\nu)^{1/2}$ versus $(h\nu)$ for monolayer $\beta\text{-In}_{2-x}\text{Al}_x\text{S}_3$ deposited on glass and realized for different percent concentration ratios of Al ($y = [\text{Al}^{3+}]/[\text{In}^{3+}]_{\text{sol}}$)

of $\beta\text{-In}_{2-x}\text{Al}_x\text{S}_3$ compound for indirect transition does not linearly increase with Al concentration. So the variation of the value of band gap for the direct transition and indirect transition can be due to Al doping which plays an important role in the optical and the structural properties of such films.

The effects of multi-layers on structural properties

The analyses being made previously allow us to conclude that $\beta\text{-In}_{2-x}\text{Al}_x\text{S}_3$ material grown on glass substrate using Al doping in starting solution $y = 4$ at.% has a best crystalline state, a dense surface morphology, a higher transparency as well as a wider band gap. For all values of y , the thickness ‘ e ’ of $\beta\text{-In}_{2-x}\text{Al}_x\text{S}_3$ is quite low and it is desirable to increase it for the better use of the $\beta\text{-In}_{2-x}\text{Al}_x\text{S}_3$ as an optical window in a solar cell. In order to increase the thickness and to obtain a good window layer in solar cell, multi-depositions of $\beta\text{-In}_{2-x}\text{Al}_x\text{S}_3$ ($y = 4$ at.%) have been prepared for three deposits. Otherwise, the layer will collapse. We also study the effect of the realization of multi-deposition thin layers on the physical properties of $\beta\text{-In}_{2-x}\text{Al}_x\text{S}_3$ material. The film thickness of layer grown after one, two, and three deposition runs measured by Dektak 3 profilometer are 400, 700, and 1200 nm, respectively. XRD patterns of $\beta\text{-In}_{2-x}\text{Al}_x\text{S}_3$ obtained for concentration ratio $y = ([\text{Al}^{3+}]/[\text{In}^{3+}])_{\text{sol}} = 4\%$ and obtained after one (1D), two (2D), and three (3D) deposition runs are shown in Fig. 5. The spectra clearly show that the crystallinity seems to be improved as the film thickness increases. The peak intensity increases with increasing deposition number and the maximum peak intensity is observed after three deposition runs. The film diffractograms (Fig. 5, 3D) displays three relatively high, sharp and well defined peaks at approximately 27.7° , 33.4° , and 48° assigned, respectively, to reticular planes (311), (400), and (440), which characterize the cubic phase of $\beta\text{-In}_2\text{S}_3$ (PDF-32-0456). The layer exhibited (400) as the preferred orientation at $2\theta = 33.4^\circ$.

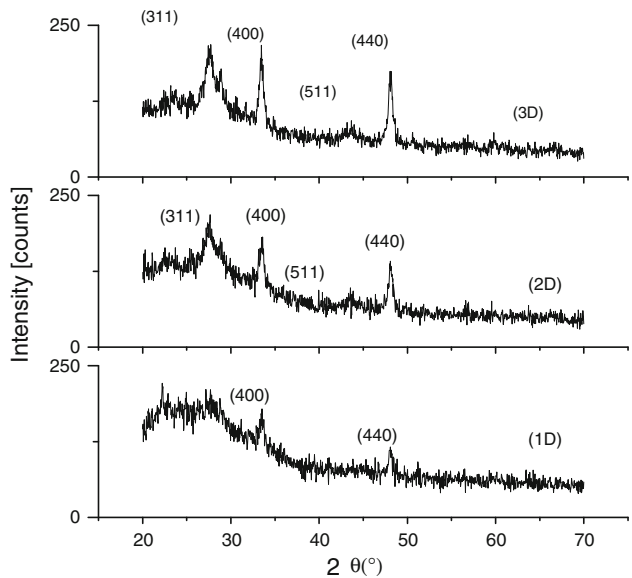


Fig. 5 X-ray patterns of $\beta\text{-In}_{2-x}\text{Al}_x\text{S}_3$ realized for $y = ([\text{Al}^{3+}]/[\text{In}^{3+}])_{\text{sol}} = 4\%$ after one (1D), two (2D), and three (3D) deposition runs

similar behavior was observed by Akkari [20] for SnS thin film, who reported that the best crystallinity is obtained after six deposition runs and by Revathi et al. [21] who reported that the intensity of In_2S_3 grown by evaporating increased with the film thickness.

To study micro-structural surface topography, SEM images have been obtained for multi-layers $\beta\text{-In}_{2-x}\text{Al}_x\text{S}_3$ deposited on glass. Figure 6 represents micrographs of the surface of the sample deposited on glass after: one, two, and three deposition runs. These images show that the

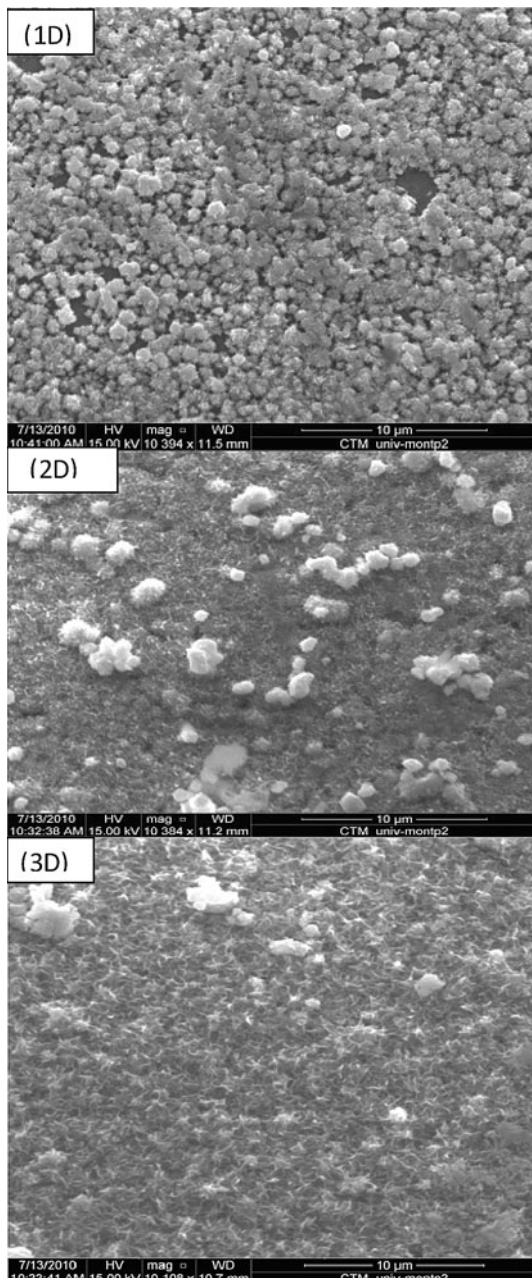


Fig. 6 Surface morphology of $\beta\text{-In}_{2-x}\text{Al}_x\text{S}_3$, grown for $y = ([\text{Al}^{3+}] / [\text{In}^{3+}]_{\text{sol}} = 4\%$, deposited on glass after: one (1D), two (2D), and three(3D) deposition runs

surface morphology of the films is strongly dependent on the layer number. In fact, after one deposition run (Fig. 6, 1D) sphere-like In_2S_3 grains are formed on glass substrate in an irregular spatial distribution and more voids can be observed, which means that some of the grains are not well developed. After two deposition runs (Fig. 6, 2D), a substantial change in surface architecture was noticed. The surface relief is indeed more compact but the spherical crystallites are uniformly distributed on the surface with the appearance of clusters. The surface morphology of $\beta\text{-In}_{2-x}\text{Al}_x\text{S}_3$ thin film prepared using content $y = 4$ at.%, after three depositions runs (Fig. 6, 3D), shows more compact structure, uniform, densely packed and continuous without any gaps or cracks. It is assumed that the surface morphology of three deposition runs is then more uniform than that of one and two deposited layers. This result is consisted with the XRD analysis which shows that the best crystalline state is therefore obtained after three deposition runs.

The effect of multi-layers on optical properties

The optical transmission (T) in the wavelength range (250–2500) nm of multi-layers $\beta\text{-In}_{2-x}\text{Al}_x\text{S}_3$ deposited on glass and realized for the concentration ratio $y = ([\text{Al}^{3+}] / [\text{In}^{3+}]_{\text{sol}} = 4\%$ is shown in Fig. 7. All samples reveal good transmission in the visible region. The optical transmittance of the films varies with the number of deposition runs. It is clearly show in the transparency and visible domain (550–900) nm that the grown film obtained after three deposition runs is more transparent ($T \approx 73\%$) than that obtained after two deposition runs ($T \approx 65\%$) this result may be correlated with the surface morphology which shows the appearance of clusters in the surface of thin film deposited after two deposition runs (Fig. 6, 2D) also XRD study show that the best crystallinity is obtained in the case of three deposition runs. Figure 7 shows a

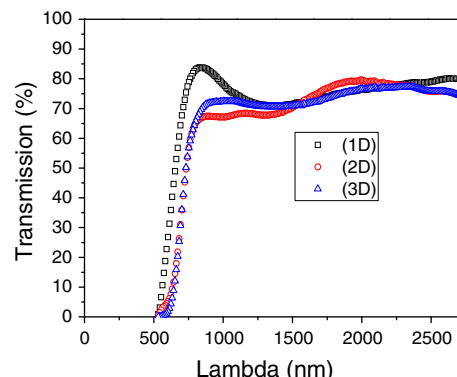


Fig. 7 Transmittance (T) of $\beta\text{-In}_{2-x}\text{Al}_x\text{S}_3$ realized for $y = ([\text{Al}^{3+}] / [\text{In}^{3+}]_{\text{sol}} = 4\%$ after one (1D), two (2D), and three(3D) deposition runs

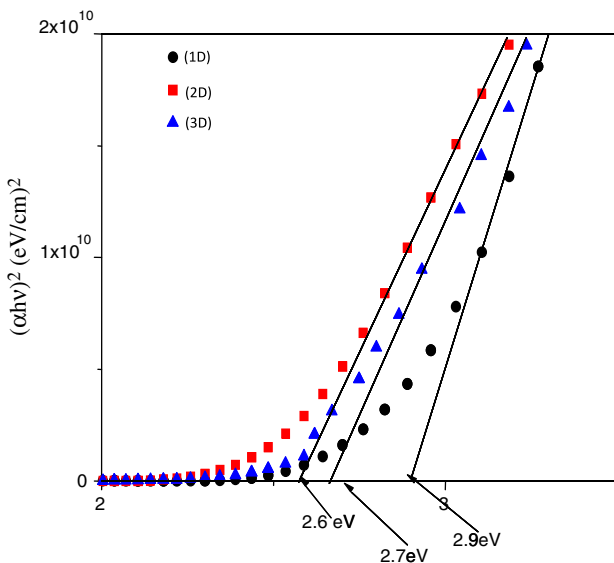


Fig. 8 Plot $(\alpha h\nu)^2$ versus $(h\nu)$ of $\beta\text{-In}_{2-x}\text{Al}_x\text{S}_3$ grown for $y = 4$ at.% on glass substrate after one (1D), two (2D), and three (3D) deposition runs

broadening and/or a shift of short-wavelength absorption edge for one deposition run which can be assigned to a disturbed state of the crystallinity of $\beta\text{-In}_{2-x}\text{Al}_x\text{S}_3$ material. The calculated of band gap energy value E_g of $\beta\text{-In}_{2-x}\text{Al}_x\text{S}_3$ multi-layers shows that E_g values are 2.9, 2.6, and 2.7 eV, respectively for (1D), (2D), and (3D). This variation may be justified by the increase of structural order Fig. 8.

Conclusion

$\beta\text{-In}_{2-x}\text{Al}_x\text{S}_3$ thin films were prepared by CBD for different percentage ratios ($0 < y = ([\text{Al}^{3+}]/[\text{In}^{3+}])_{\text{sol}} < 5$ at.%). The obtained results confirm that the variation of Al concentration has an effect on the growth of layer, on the structure and especially on the value of band gap. So two energy band gap were determined: one direct for all layers and other indirect only for $y = 1, 2$, and 5 at.%. The XRD analyses show that the best crystallinity was obtained for ratio $y = 4$ and 5 at.%. However, the optical analysis revealed that the higher transmission ($T \approx 75\%$) and the wider band gap ($E_g \approx 2.9$ eV) were obtained for the ratio $y = 4$ at.%, these results allow us to conclude that the optimum level is obtained for $y = 4$ at.%. So in order to improve the thickness and the physical properties of $\beta\text{-In}_{2-x}\text{Al}_x\text{S}_3$ we study the multi-depositions system. The X-ray analysis revealed that the better crystallinity was obtained after three deposition runs, the morphological analysis approves those obtained by XRD. The evaluation of the optical properties of thin films $\beta\text{-In}_{2-x}\text{Al}_x\text{S}_3$ obtained after

three deposition runs showed a well transmission at about 73% and the optical gap is of around 2.7 eV which justifies its utilization as optical window layer in the solar cell in photovoltaic system such as $\text{Au}/\text{CuInS}_2/\beta\text{-In}_{2-x}\text{Al}_x\text{S}_3/\text{SnO}_2$ in which CuInS_2 is used as an absorber material and $\text{SnO}_2:\text{F}$ as an ohmic contact. CuInS_2 and SnO_2 have been grown in our laboratory by Spray pyrolysis technique [22, 23].

It is important to conclude that the CBD technique allows the synthesis of good $\beta\text{-In}_{2-x}\text{Al}_x\text{S}_3$ thin films. Moreover, we are intend to improve the physical properties of this material by carrying out either heat treatment under different temperatures or by doping $\beta\text{-In}_2\text{S}_3$ by different other elements to reach the best performance of window based on doped In_2S_3 binary materials for future thin film-solar cell.

Acknowledgements The authors would like to thank Dr. C. Guash from Institut d'Electronique du Sud, Université de Montpellier II, and Pr. M. Amlouk from Unité de Physique des Dispositifs à Semiconducteurs, Faculté des Sciences de Tunis for help.

References

1. Lajnef M, Ezzouia H (2009) Open Appl Phys J 22:23
2. Barreau N, Marsillac S, Bernède JC (2000) Vacuum 56:101
3. Theresa John T, Bini S, Kashiwabara Y, Abe T, Yasuhiro Y, Sudha Kartha C, Vijayakumar KP (2003) Semicond Sci Technol 18:491
4. Braunger D, Hariskos D, Waltre T, Schock HW (1996) Sol Energy Mater Sol Cells 40:97
5. Theresa John T, Meril M, Sudha Kartha C, Vijayakumar KP, Abeb T, Kashiwabab Y (2005) Sol Energy Mater Sol Cells 89:27
6. Li Z, Tao X, Wu Z, Zhang P, Zhang Z (2009) Ultrason Sonochem 16:221
7. Asenjo B, Sanz C, Guillén C, Chaparro AM, Gutiérrez MT, Herrero J (2007) Thin Solid Films 515:6041
8. Lokhande CD, Ennaoui A, Patil PS, Giersig M, Diesner K, Muller M, Tributsch H (1999) Thin Solid Films 340:18
9. Barreau N, Bernede JC, Deudon C, Brohen L, Marsillac S (2002) Thin Solid Films 241:4
10. Barreau N (2009) Sol Energy 83:363
11. Mathew M, Gopinath M, Kartha CS, Vijayakumar KP, Kashiwaba Y, Abe T (2010) Sol Energy 84:888
12. Meril M, Sudha Kartha C, Vijayakumar KP (2009) J Mater Sci 20:294. doi:[10.1007/s10854-008-9591-7](https://doi.org/10.1007/s10854-008-9591-7)
13. Ho C-H (2010) J Cryst Growth 312:2718
14. Kamoun N, Belgacem S, Amlouk M, Bennaceur R, Bonnet J, Touhari F, Nouaoura M, Lassabatere L (2001) J Appl Phys 89:2766
15. Yahmadi B, Kamoun N, Bennaceur R, Mnari M, Dachraoui M, Abdelkrim K (2005) Thin Solid Films 473:201
16. Couzinié-Devy F, Arzel L, Barreau N, Guillot-Dedon C, harel S, Lafond A, Kessler J (2010) J Cryst Growth 312:502
17. Eberhart JP (1989) Analyse structurale et chimique des matériaux. Dunod, Paris, p 231
18. Pankove JI (1971) Optical process in semiconductors. Dover Publication, New York
19. Sandoval-Paz MG, Sotelo-Lerma M, Valenzuela-Jáuregui JJ, Flores-Acosta M, Ramrez-Bon R (2005) Thin Solid Films 472:5

20. Akkari A, Guasch C, Kamoun-Turki N (2010) J Alloys Comp 490:180
21. Revathi N, Prathap P, Ramakrishna Reddy KT (2009) Solid State Sci 11:1288
22. Kamoun N, Jebbari N, Belgacem S, Bennaceur R (2002) J Appl Phys 91:1952
23. belgacem S, Bennaceur R (1990) Revue Phys Appl 25:1245